

Integrating transcriptome-wide association studies with gene co-expression patterns

Draft manuscript

Text in red/red are internal comments

This manuscript ([permalink](#)) was automatically generated from [greenelab/phenoplier_manuscript@1cfa19a](#) on March 16, 2021.

Authors

- **Milton Pivodori**

 [0000-0002-3035-4403](#) ·  [miltondp](#) ·  [miltondp](#)

Department of Systems Pharmacology and Translational Therapeutics, Perelman School of Medicine, University of Pennsylvania, Philadelphia, PA 19104, USA · Funded by The Gordon and Betty Moore Foundation GBMF 4552; The National Human Genome Research Institute (R01 HG010067)

- **Marylyn D. Ritchie**

 [0000-0002-1208-1720](#) ·  [MarylynRitchie](#)

Department of Genetics, Perelman School of Medicine, University of Pennsylvania, Philadelphia, PA, USA

- **Casey S. Greene**

 [0000-0001-8713-9213](#) ·  [cgreene](#) ·  [GreeneScientist](#)

Center for Health AI, University of Colorado School of Medicine, Aurora, CO, 80045, USA; Department of Biochemistry and Molecular Genetics, University of Colorado School of Medicine, Aurora, CO, 80045, USA · Funded by The Gordon and Betty Moore Foundation (GBMF 4552); The National Human Genome Research Institute (R01 HG010067); The National Cancer Institute (R01 CA237170)

Abstract

Results

PhenoPLIER integrates TWAS with gene co-expression patterns

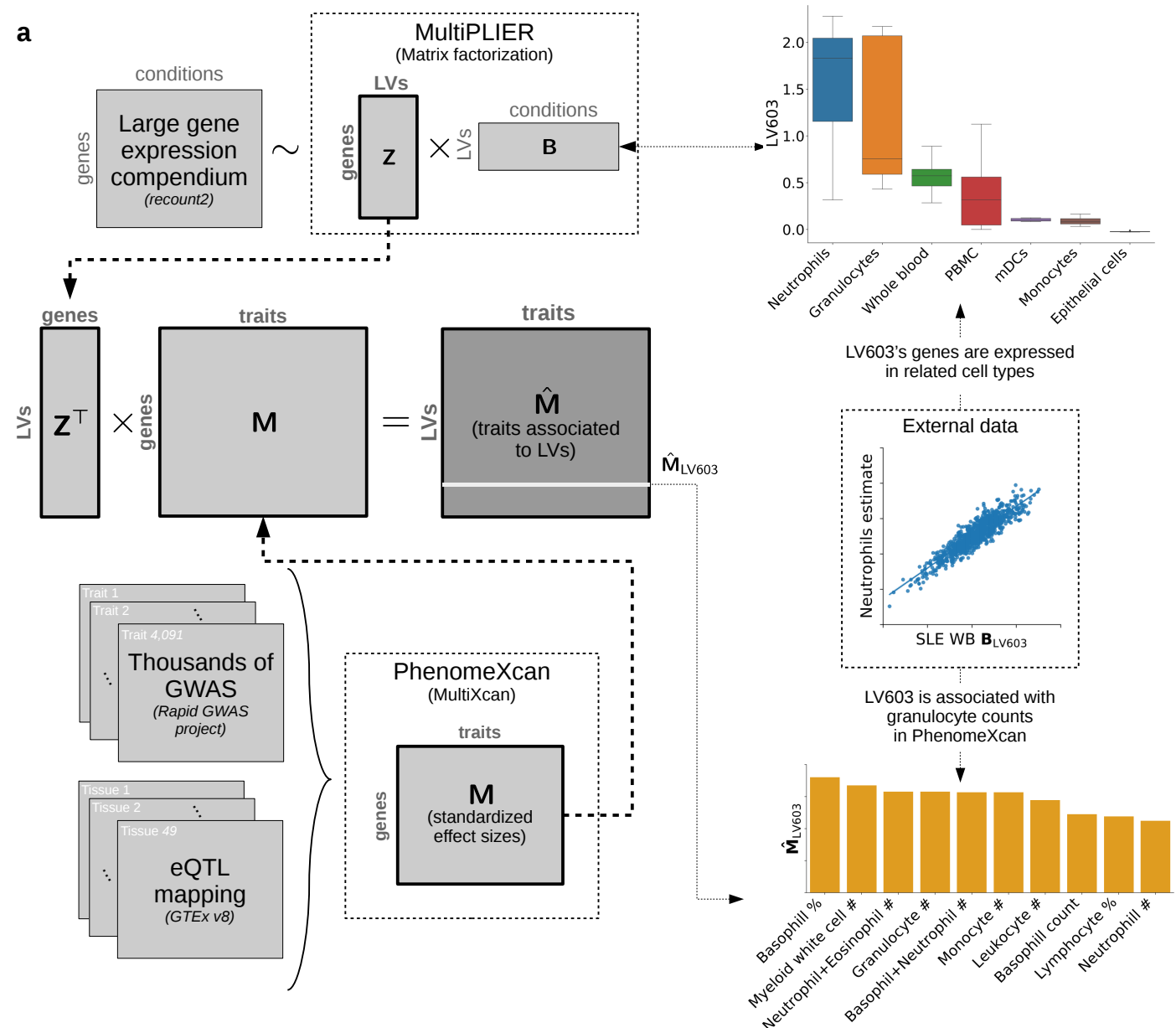


Figure 1: Schematic of the PhenoPLIER framework. a) The integration process between gene co-expression patterns from MultiPLIER [1] (top) and TWAS results from PhenomeXcan [2]. PhenoPLIER projects gene-based association results on ~4,000 traits to a latent space learned from a large gene expression compendium (recount2 [3]). This generates matrix \hat{M} , where each trait is now described by latent variables/gene modules. **b)** After the integration process, we found that neutrophil counts and other white blood cells (bottom) were ranked among the top 10 traits for an LV that was termed a neutrophil signature in the original MultiPLIER study. Genes in this LV were found to be expressed in relevant cell types (top). PMBC: [Explain](#); mDCs: [Explain](#).

(This paragraph has probably too much detail about MultiPLIER) MultiPLIER [1] is a recent computational strategy that extracts patterns of co-expressed genes from large gene expression datasets. The approach uses an unsupervised matrix factorization method that was employed to extract latent variables from recount2 [3]. The latent variables (LVs), essentially gene modules, then revealed biological processes associated with disease severity in rare disease datasets

that were too small for effective model training. These gene sets aligned well with known biological pathways and predicted cell type composition, even though the approach was not explicitly designed for this goal.

Although the authors showed that certain patterns learned by MultiPLIER resemble known biology, most of the LVs identified are completely unknown. Since genes in these modules vary together in certain cell types and tissues, it's expected that they may also function together [4,5]. To test whether patterns in the expression space match those in the TWAS space, we used PhenomeXcan [2], a massive transcriptome-wide association studies (TWAS) resource obtained from the UK Biobank [6] and other cohorts (Figure 1 a). These results were projected to the low-dimensional gene representation learned by MultiPLIER using:

$$\hat{\mathbf{M}} = (\mathbf{Z}^\top \mathbf{Z} + \lambda_2 \mathbf{I})^{-1} \mathbf{Z}^\top \mathbf{M}, \quad (1)$$

where $\mathbf{M}^{n \times t}$ has gene-trait associations from MultiXcan [7] (standardized effect sizes) for n genes and t traits, $\mathbf{Z}^{n \times l}$ are the gene loadings with l latent variables, λ_2 is the regularization parameter used in the training step, and $\hat{\mathbf{M}}^{l \times t}$ is finally the projection of \mathbf{M} into the latent space: all traits in PhenomeXcan are now described by LVs, thus we can potentially infer the effects of gene modules on different human traits. Since the MultiPLIER models also provide the experimental conditions (such as cell types and tissues) in which genes in a module are concurrently expressed, our approach would also allow inferring the context in which the gene module affects a trait or disease.

In the original MultiPLIER study [1], the authors found an LV significantly associated with previously known neutrophil gene-sets and highly correlated with neutrophil estimates from gene expression. We analyzed this LV using our approach (Figure 1 b), and found that 1) neutrophil counts and other white blood cell traits from PhenomeXcan [2] were ranked among the top 10 traits for this LV, and 2) that the genes in this LV are expressed in neutrophil cells (see more details in the supplementary material). These initial results strongly suggest that shared patterns exist in the gene expression space (which has no GTEx samples) and the TWAS space (with gene models trained using GTEx v8), and that the approach also allows to infer the context-specific effects of gene modules on complex traits. We will also show how the approach can aid translational efforts by mapping pharmacological perturbations to this latent space, enabling to observe which compounds affect the transcriptional activity of gene modules.

- Minor: LV603 is neutrophil-associated, but it is not significantly associated with other myeloid lineage cell types (see Figure S2A in MultiPLIER study). Maybe we can add a genes-traits figure of MultiXcan and fastENLOC results to see this better.

Clusters of traits in the gene module space are associated with relevant transcriptional processes

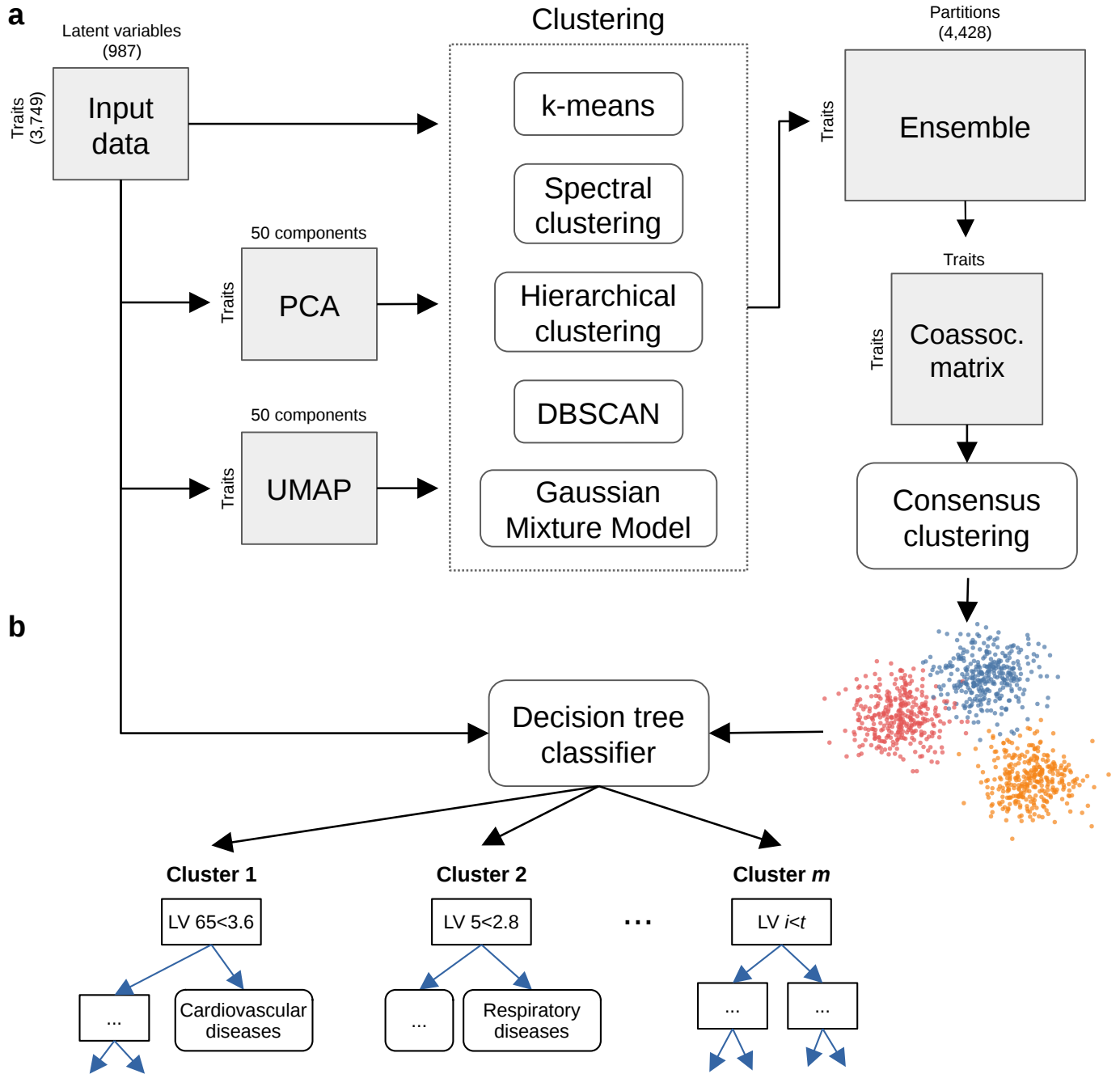


Figure 2: Cluster analysis on traits from PhenomeXcan. a) The projection of TWAS results for 3,749 traits to the latent representation learned from recount2 are the input data to the clustering process. A linear (PCA) and non-linear (UMAP) dimensionality reduction techniques are applied to the input data, and the three data versions are processed by five different clustering algorithms. These algorithms derive partitions from the data using different sets of parameters (such as the number of clusters), leading to an ensemble of 4,428 partitions. A coassociation matrix is derived by counting how many times a pair of traits were grouped together in the ensemble. Finally, a consensus function is applied to the coassociation matrix to generate consolidated partitions with different number of clusters. These final solutions are represented in the clustering tree (Figure 3). **b)** The clusters found by the consensus function are used as labels to train a decision tree classifier on the original input data, which detects the most important LVs that differentiate groups of traits.

All traits in PhenomeXcan were projected into the latent space learned from recount2 using Equation (1). We conducted cluster analysis using this new representation to find groups of traits that are similarly affected by the same transcriptional processes. To avoid using a single clustering algorithm (which implies using a single assumption about the structure of the data), we employed a consensus clustering approach where different methods with varying sets parameters are applied on the same data, and later combined into a consolidated solution [8,9,10] (Figure 2). An important property for a successful application of a consensus clustering approach is the diversity of the ensemble, understood as the level of disagreement between the base clustering solutions [8,11,12]. A diverse

set of solutions can be generated by using different data representations (such as dimensionality reduction methods or subsets of features), clustering algorithms with distinct assumptions (k -means, for instance, assumes hyperspherical clusters), and a varying set of algorithm's parameters (such as the number of clusters or the initial random seeds). In our approach, we performed cluster analysis using five different clustering algorithms on three representations of the input data (the original data with 987 latent variables, its projection into the top 50 principal components, and the embedding learned by UMAP [13] using 50 components) (see Figure 2 a). The clustering methods used cover a wide range of different assumptions on cluster shapes and a varying set of parameters such as the number of clusters (from 2 to 60), the width of the Gaussian kernel in spectral clustering, and other method-specific parameters (see the supplementary material for more details). The process generated an ensemble with 4,428 clustering solutions for all traits. This ensemble was used to derive a coassociation matrix between traits by counting the number of times a pair of traits was clustered together. A consensus function was applied on the coassociation matrix to derive a consolidated solution using the information in the ensemble. For these final partitions, we did not select a specific number of clusters, but instead used a clustering tree [14] (Figure 3) to examine stable groups of traits at multiple resolutions. Finally, for the interpretation of the clusters, we trained a decision tree classifier (a highly interpretable machine learning model) on the original input data using the clusters found as labels. This approach allowed us to quickly identify the most important gene modules for the groups of traits found. More details of the clustering process are available in the supplementary material.

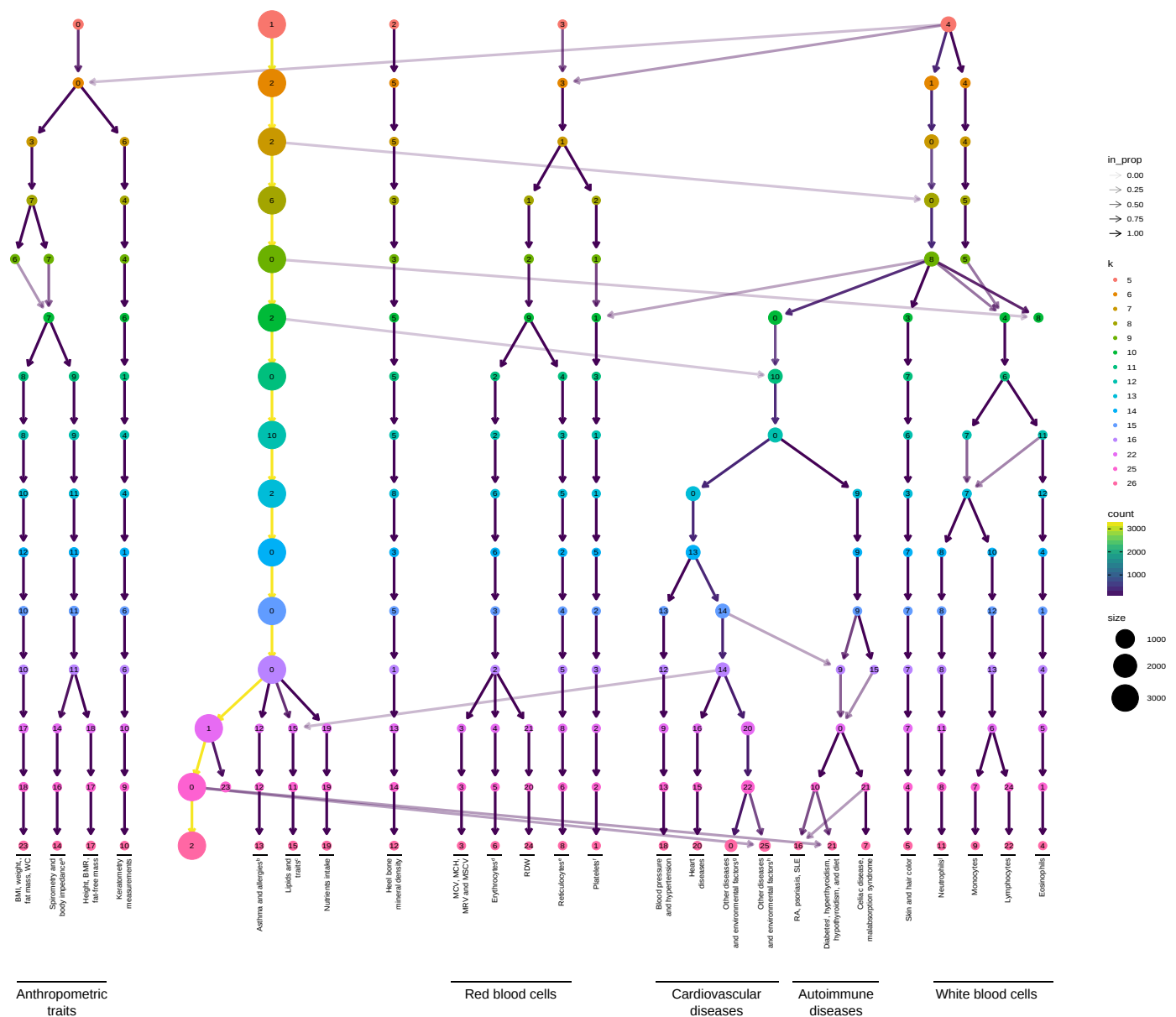


Figure 3: Clustering tree using multiple resolutions. Clustering tree of the consensus partitions at different resolutions (from 5 to 26 clusters). Each row represents a partition of the traits, and each circle is a cluster from that partition. Arrows indicate how traits in one cluster move across clusters from different partitions. Some clusters, such as anthropometric traits, blood cell counts, and some complex diseases are highly stable across different resolutions. BMR: basal metabolic rate; WC: waist/hip circumference; MCV: mean corpuscular volume; MCH: mean corpuscular hemoglobin; MRV: mean reticulocyte volume; MSCV: mean spherized cell volume; RDW: red cell (erythrocyte) distribution width; RA: rheumatoid arthritis; SLE: systemic lupus erythematosus; ^a includes whole-body, arms and legs impedances; ^b allergies refer to allergic rhinitis or atopic dermatitis; ^c includes Alzheimer's disease, coronary artery disease, breast cancer, fasting blood glucose and insulin measurements, inflammatory bowel disease, and atopic dermatitis; ^d includes erythrocyte count, hemoglobin concentration, and hematocrit percentage; ^e includes reticulocyte count and percentage, immature reticulocyte fraction, and high light scatter reticulocytes count and percentage; ^f includes platelet count, platelet crit, mean platelet volume, and platelet distribution width. ^g includes diabetes, gout, arthrosis, and respiratory diseases (and related medications such as ramipril, allopurinol, lisinopril, and albuterol), and several environmental/behavioral factors such as: intake of a range of common food/drink items including alcohol, time spent outdoors and watching TV, smoking and sleeping habits, early-life factors, education attainment, psychological and mental health, and health satisfaction. ^h includes vascular problems such as angina, deep vein thrombosis (DVT), intraocular pressure, eye and mouth problems, hand grip strength, several measurements of physical activity, jobs involving heavy physical work, transport type for commuting, intake of common vitamin/mineral supplements, and various types of body pain and medications for pain relief. ⁱ age when diabetes was first diagnosed; ^j includes neutrophil count, neutrophil+basophil count, neutrophil+eosinophil count, granulocyte count, leukocyte count, and myeloid cell count.

A clustering tree of the consensus solutions at different resolutions is shown in Figure 3. For each k (the number of clusters), the consensus partition that maximized the agreement with the ensemble was selected (see supplementary material). Since it is expected that a subset of resolutions better represents the patterns among traits, we further filtered the consensus partitions by taking those with an agreement value higher than the 75th percentile, which included partitions from 4 to 45 clusters.

- mention that some clusters, like 25, 16, and 21 (diabetes and autoimmunity) are “unstable”.
- this shows the complexity of autoimmune diseases in this data representation
- the arrows that go out and in in the “complex” branch to the other branches show the complexity of connection for some traits; MAYBE I CAN MENTION SOME HERE.

The clustering tree shows four clear branches (from right to left): results from hematological assays (blood cell count), anthropometric traits, bone-densitometry of heel and keratometry measurements, and the “complex” branch. The first three branches include highly stable clusters, where the same traits are clustered together across different resolutions and different random seeds in the consensus clustering algorithm. The complex branch also includes stable clusters at different resolutions, such as 1) skin and hair color, 2) blood pressure and hypertension, 3) asthma, allergic rhinitis, and atopic dermatitis, 4) cardiovascular diseases (coronary artery disease, myocardial infarction, angina pectoris, among others) and related medications, 5) schizophrenia, educational outcomes, and fluid intelligence score 6) autoimmune diseases (celiac disease, hypothyroidism, psoriasis, rheumatoid arthritis, systemic lupus erythematosus, type 1 diabetes, among others), 7) breath spirometry, 8) nutrients intake, 9) lipids and Alzheimer's disease, 10) intraocular pressure (cornea), 11) smoking habits, and 12) happiness and well-being. In the following sections, we selected some of these stable clusters to analyze the transcriptional processes that differentiate them.

- Maybe include Ben's question about why we expect these clustering results. My answer was more or less that far apart clusters are explained by more specific LVs to those traits, and the complex branch is more related to traits that are highly connected to all biological processes, where more subtle differences are captured only at higher resolutions.

Cardiovascular traits

See if we are going to analyze this cluster.

The figures below include examples of the type of figure we can include here:

- Show the LVs that are distinct for this cluster (maybe a small decision tree for some of the clusters).
- For those LV, show which cell types/tissues are important (such as Figure 4 below).
- For some of these LVs, we can include the list of other traits also related and gene association results (such as Figure 5).

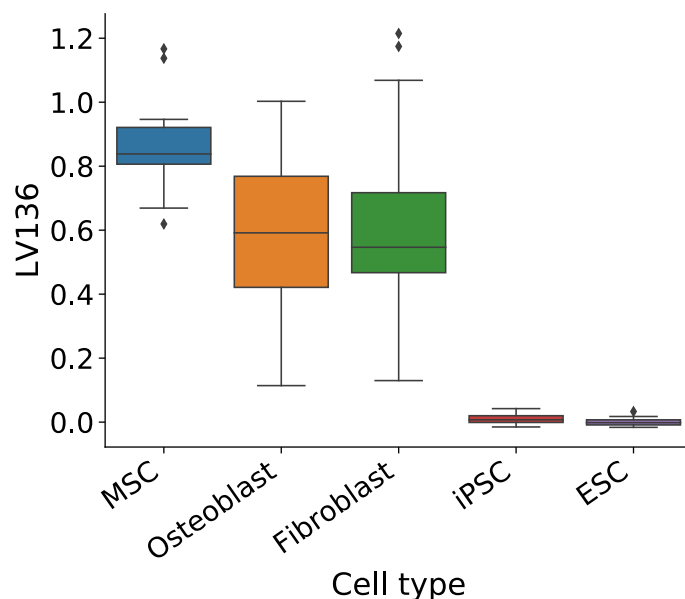


Figure 4: Cell types/tissues associated with genes in LV136.

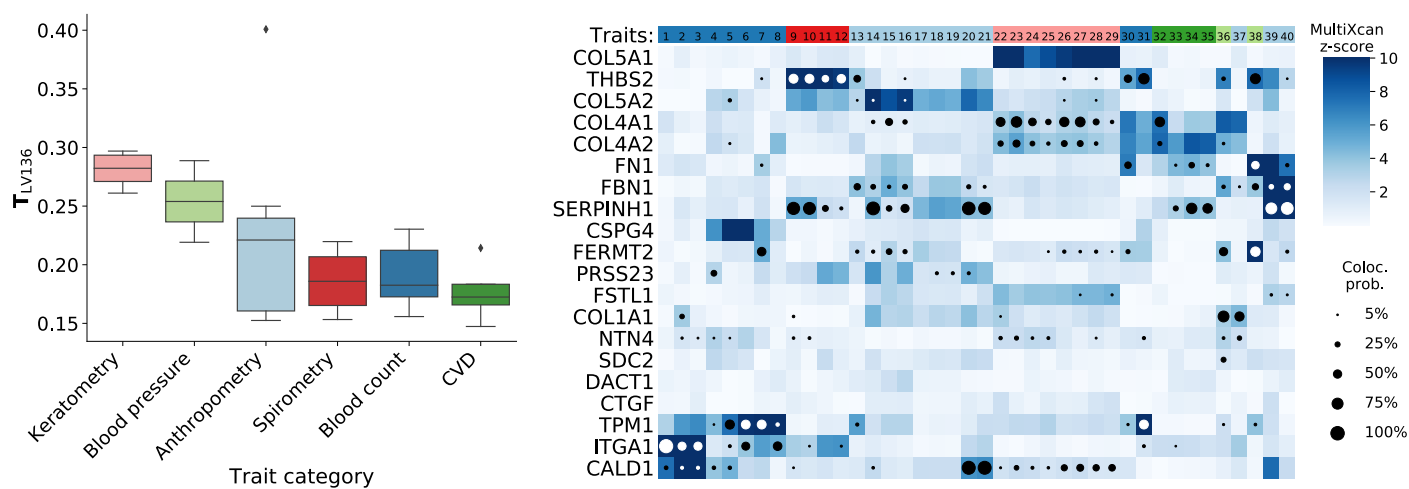


Figure 5: Traits associated with genes in LV136.

Schizophrenia, educational attainment and intelligence

See if we are going to analyze this cluster.

Asthma and allergies

See if we are going to analyze this cluster.

Replication using Penn Medicine BioBank

Maybe we can incorporate **Binglan's TWAS results on PMBB** and see if expected traits-clusters are correctly predicted.

PhenoPLIER improves drug-disease prediction

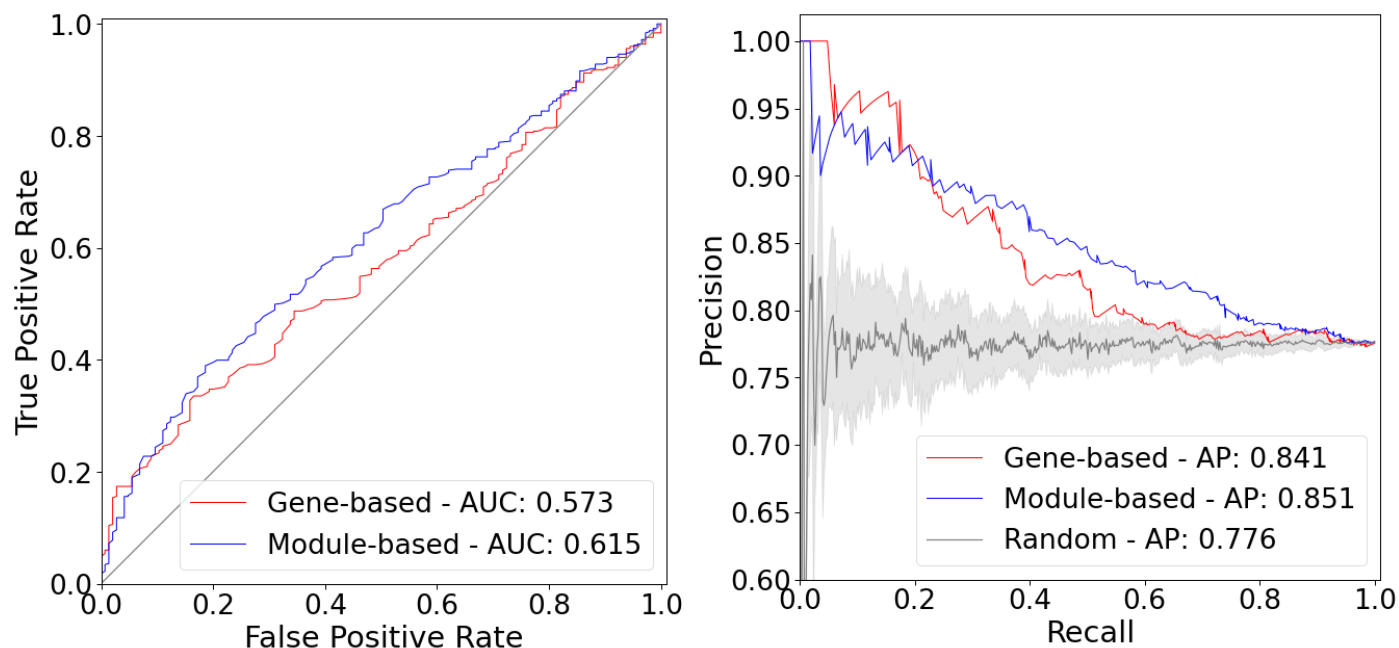


Figure 6: Drug-disease prediction. Explain. AUC: area under the curve; AP: average precision.

We showed that the latent representation learned in a large gene expression data set is helpful to link novel gene sets to complex diseases and the cell types where they are expressed. We reasoned that this representation might be also useful to more accurately predict the potential therapeutic effects of drugs. If the gene patterns captured by MultiPLIER represent real and possibly unknown biological pathways, then our approach might actually produce a more accurate estimation of the effects of a perturbed molecular mechanisms on disease, and also how pharmacological perturbations affect the process activity. This would, in addition to connecting gene modules with their context-specific effects on complex traits, identify which compounds might provide an avenue to alter a dysregulated process activity for therapeutical utility.

To test this hypothesis, we used a gold standard of drug-disease medical indications [15,16] to evaluate and compare the prediction performance of both the original gene-disease associations from PhenomeXcan, and its projection representing gene module-disease associations. To test this, we used the transcriptional responses to small molecule perturbations profiled in LINCS L1000 [17], which were further processed to obtain consensus signatures and map to DrugBank IDs [15,18,19]. To compute a drug-disease score, we followed a similar procedure used previously [20] to anti-correlates gene-traits associations from TWAS and expression profiles of drugs using their signed z -scores (see the supplementary material). Here we used the dot product between gene-traits z -scores and the consensus z -scores in LINCS L1000, which led to a score for each drug-disease pair. (Add more details?). To obtain a drug-disease association for the gene module-mapped TWAS results, we first projected LINCS L1000 data into this latent representation using Equation (1), thus leading to a matrix with the expression profiles of drugs mapped to latent variables. This can be interpreted as the effects of compounds on gene modules activity. Then, similarly as before, we anti-correlated gene module-traits scores and module expression profiles of drugs.

(Add number of drugs, diseases, and final number of mappings)

The ROC and Precision-Recall (PR) curves comparing both approaches are shown in Figure 6. Notably, the gene module-based approach proposed here clearly outperformed the gene-based one, with an area under the curve (AUC) of 0.615 vs 0.573, and an average precision (AP) of 0.851 vs 0.841. This is particularly striking given that the projected TWAS results represent a reduced or compressed version

of the complete gene-based associations, suggesting that a gene module perspective can be more informative, for instance, for drug-repurposing scenarios using genetic studies.

Another analysis here could be:

- Try the prediction again by keeping well-aligned LVs only. Do we get the same prediction performance?

Discussion

References

1. MultiPLIER: A Transfer Learning Framework for Transcriptomics Reveals Systemic Features of Rare Disease

Jaclyn N. Taroni, Peter C. Grayson, Qiwen Hu, Sean Eddy, Matthias Kretzler, Peter A. Merkel, Casey S. Greene

Cell Systems (2019-05) <https://doi.org/gf75g5>

DOI: [10.1016/j.cels.2019.04.003](https://doi.org/10.1016/j.cels.2019.04.003) · PMID: [31121115](https://pubmed.ncbi.nlm.nih.gov/31121115/) · PMCID: [PMC6538307](https://pubmed.ncbi.nlm.nih.gov/PMC6538307/)

2. PhenomeXcan: Mapping the genome to the phenome through the transcriptome

Milton Pividori, Padma S. Rajagopal, Alvaro Barbeira, Yanyu Liang, Owen Melia, Lisa Bastarache, YoSon Park, GTEx Consortium, Xiaoquan Wen, Hae K. Im

Science Advances (2020-09) <https://doi.org/ghbvbf>

DOI: [10.1126/sciadv.aba2083](https://doi.org/10.1126/sciadv.aba2083) · PMID: [32917697](https://pubmed.ncbi.nlm.nih.gov/32917697/)

3. Reproducible RNA-seq analysis using recount2

Leonardo Collado-Torres, Abhinav Nellore, Kai Kammers, Shannon E Ellis, Margaret A Taub, Kasper D Hansen, Andrew E Jaffe, Ben Langmead, Jeffrey T Leek

Nature Biotechnology (2017-04-11) <https://doi.org/gf75hp>

DOI: [10.1038/nbt.3838](https://doi.org/10.1038/nbt.3838) · PMID: [28398307](https://pubmed.ncbi.nlm.nih.gov/28398307/) · PMCID: [PMC6742427](https://pubmed.ncbi.nlm.nih.gov/PMC6742427/)

4. Finding function: evaluation methods for functional genomic data

Chad L Myers, Daniel R Barrett, Matthew A Hibbs, Curtis Huttenhower, Olga G Troyanskaya

BMC Genomics (2006-07-25) <https://doi.org/fg6wnk>

DOI: [10.1186/1471-2164-7-187](https://doi.org/10.1186/1471-2164-7-187) · PMID: [16869964](https://pubmed.ncbi.nlm.nih.gov/16869964/) · PMCID: [PMC1560386](https://pubmed.ncbi.nlm.nih.gov/PMC1560386/)

5. The CAFA challenge reports improved protein function prediction and new functional annotations for hundreds of genes through experimental screens

Naihui Zhou, Yuxiang Jiang, Timothy R. Bergquist, Alexandra J. Lee, Balint Z. Kacsóh, Alex W.

Crocker, Kimberley A. Lewis, George Georgioui, Huy N. Nguyen, Md Nafiz Hamid, ... Iddo Friedberg

Genome Biology (2019-11-19) <https://doi.org/ggnxpz>

DOI: [10.1186/s13059-019-1835-8](https://doi.org/10.1186/s13059-019-1835-8) · PMID: [31744546](https://pubmed.ncbi.nlm.nih.gov/31744546/) · PMCID: [PMC6864930](https://pubmed.ncbi.nlm.nih.gov/PMC6864930/)

6. The UK Biobank resource with deep phenotyping and genomic data

Clare Bycroft, Colin Freeman, Desislava Petkova, Gavin Band, Lloyd T. Elliott, Kevin Sharp, Allan Motyer, Damjan Vukcevic, Olivier Delaneau, Jared O'Connell, ... Jonathan Marchini

Nature (2018-10-10) <https://doi.org/gfb7h2>

DOI: [10.1038/s41586-018-0579-z](https://doi.org/10.1038/s41586-018-0579-z) · PMID: [30305743](https://pubmed.ncbi.nlm.nih.gov/30305743/) · PMCID: [PMC6786975](https://pubmed.ncbi.nlm.nih.gov/PMC6786975/)

7. Integrating predicted transcriptome from multiple tissues improves association detection

Alvaro N. Barbeira, Milton Pividori, Jiamao Zheng, Heather E. Wheeler, Dan L. Nicolae, Hae Kyung Im

PLOS Genetics (2019-01-22) <https://doi.org/ghs8vx>

DOI: [10.1371/journal.pgen.1007889](https://doi.org/10.1371/journal.pgen.1007889) · PMID: [30668570](https://pubmed.ncbi.nlm.nih.gov/30668570/) · PMCID: [PMC6358100](https://pubmed.ncbi.nlm.nih.gov/PMC6358100/)

8. Diversity control for improving the analysis of consensus clustering

Milton Pividori, Georgina Stegmayer, Diego H. Milone

Information Sciences (2016-09) <https://doi.org/ghtqbk>

DOI: [10.1016/j.ins.2016.04.027](https://doi.org/10.1016/j.ins.2016.04.027)

9. Clustering ensembles: models of consensus and weak partitions

A. Topchy, A. K. Jain, W. Punch

IEEE Transactions on Pattern Analysis and Machine Intelligence (2005-12) <https://doi.org/c8z32x>

DOI: [10.1109/tpami.2005.237](https://doi.org/10.1109/tpami.2005.237) · PMID: [16355656](https://pubmed.ncbi.nlm.nih.gov/16355656/)

10. Cluster Ensembles – A Knowledge Reuse Framework for Combining Multiple Partitions

Alexander Strehl, Ghosh Joydeep

Journal of Machine Learning Research <https://www.jmlr.org/papers/v3/strehl02a.html>

11. A Link-Based Approach to the Cluster Ensemble Problem

Natthakan Iam-On, Tossapon Boongoen, Simon Garrett, Chris Price

IEEE Transactions on Pattern Analysis and Machine Intelligence (2011-12) <https://doi.org/cqgkh3>

DOI: [10.1109/tpami.2011.84](https://doi.org/10.1109/tpami.2011.84) · PMID: [21576752](https://pubmed.ncbi.nlm.nih.gov/21576752/)

12. Hybrid clustering solution selection strategy

Zhiwen Yu, Le Li, Yunjun Gao, Jane You, Jiming Liu, Hau-San Wong, Guoqiang Han

Pattern Recognition (2014-10) <https://doi.org/ghtzwt>

DOI: [10.1016/j.patcog.2014.04.005](https://doi.org/10.1016/j.patcog.2014.04.005)

13. UMAP: Uniform Manifold Approximation and Projection for Dimension Reduction

Leland McInnes, John Healy, James Melville

arXiv (2020-09-21) <https://arxiv.org/abs/1802.03426>

14. Clustering trees: a visualization for evaluating clusterings at multiple resolutions

Luke Zappia, Alicia Oshlack

GigaScience (2018-07) <https://doi.org/gfzqf5>

DOI: [10.1093/gigascience/giy083](https://doi.org/10.1093/gigascience/giy083) · PMID: [30010766](https://pubmed.ncbi.nlm.nih.gov/30010766/) · PMCID: [PMC6057528](https://pubmed.ncbi.nlm.nih.gov/PMC6057528/)

15. Systematic integration of biomedical knowledge prioritizes drugs for repurposing

Daniel Scott Himmelstein, Antoine Lizée, Christine Hessler, Leo Brueggeman, Sabrina L Chen, Dexter Hadley, Ari Green, Pouya Khankhanian, Sergio E Baranzini

eLife (2017-09-22) <https://doi.org/cdfk>

DOI: [10.7554/elife.26726](https://doi.org/10.7554/elife.26726) · PMID: [28936969](https://pubmed.ncbi.nlm.nih.gov/28936969/) · PMCID: [PMC5640425](https://pubmed.ncbi.nlm.nih.gov/PMC5640425/)

16. Dhimmel/Indications V1.0. Pharmacotherapydb: The Open Catalog Of Drug Therapies For Disease

Daniel S. Himmelstein, Pouya Khankhanian, Christine S. Hessler, Ari J. Green, Sergio E. Baranzini

Zenodo (2016-03-15) <https://doi.org/f3mqwb>

DOI: [10.5281/zenodo.47664](https://doi.org/10.5281/zenodo.47664)

17. A Next Generation Connectivity Map: L1000 Platform and the First 1,000,000 Profiles

Aravind Subramanian, Rajiv Narayan, Steven M. Corsello, David D. Peck, Ted E. Natoli, Xiaodong Lu, Joshua Gould, John F. Davis, Andrew A. Tubelli, Jacob K. Asiedu, ... Todd R. Golub

Cell (2017-11) <https://doi.org/cgwt>

DOI: [10.1016/j.cell.2017.10.049](https://doi.org/10.1016/j.cell.2017.10.049) · PMID: [29195078](https://pubmed.ncbi.nlm.nih.gov/29195078/) · PMCID: [PMC5990023](https://pubmed.ncbi.nlm.nih.gov/PMC5990023/)

18. DrugBank 4.0: shedding new light on drug metabolism

Vivian Law, Craig Knox, Yannick Djoumbou, Tim Jewison, An Chi Guo, Yifeng Liu, Adam Maciejewski, David Arndt, Michael Wilson, Vanessa Neveu, ... David S. Wishart

Nucleic Acids Research (2014-01) <https://doi.org/f3mn6d>

DOI: [10.1093/nar/gkt1068](https://doi.org/10.1093/nar/gkt1068) · PMID: [24203711](https://pubmed.ncbi.nlm.nih.gov/24203711/) · PMCID: [PMC3965102](https://pubmed.ncbi.nlm.nih.gov/PMC3965102/)

19. Dhimmel/Lincs V2.0: Refined Consensus Signatures From Lincs L1000

Daniel Himmelstein, Leo Brueggeman, Sergio Baranzini

Zenodo (2016-03-08) <https://doi.org/f3mqvr>

DOI: [10.5281/zenodo.47223](https://doi.org/10.5281/zenodo.47223)

20. Analysis of genome-wide association data highlights candidates for drug repositioning in psychiatry

Hon-Cheong So, Carlos Kwan-Long Chau, Wan-To Chiu, Kin-Sang Ho, Cho-Pong Lo, Stephanie Ho-Yue Yim, Pak-Chung Sham

Nature Neuroscience (2017-08-14) <https://doi.org/gbrssh>

DOI: [10.1038/nn.4618](https://doi.org/10.1038/nn.4618) · PMID: [28805813](https://pubmed.ncbi.nlm.nih.gov/28805813/)

21. Pathway-level information extractor (PLIER) for gene expression data

Weiguang Mao, Elena Zaslavsky, Boris M. Hartmann, Stuart C. Sealfon, Maria Chikina

Nature Methods (2019-06-27) <https://doi.org/gf75g6>

DOI: [10.1038/s41592-019-0456-1](https://doi.org/10.1038/s41592-019-0456-1) · PMID: [31249421](https://pubmed.ncbi.nlm.nih.gov/31249421/) · PMCID: [PMC7262669](https://pubmed.ncbi.nlm.nih.gov/PMC7262669/)

Supplementary material

Pathway-level information extractor (PLIER)

MultiPLIER [[1](#)], the computational strategy used in this work, extracts patterns of co-expressed genes on large gene expression datasets. MultiPLIER applies the pathway-level information extractor method (PLIER) [[21](#)] to the recount2 data [[3](#)], which performs unsupervised learning using prior knowledge to reduce technical noise. Via a matrix factorization approach, PLIER deconvolutes the gene expression data into a set of latent variables (LV) that each represent a gene module (i.e. a set of genes with coordinated expression patterns).

COMPLETE

Top latent variables associated to neutrophils

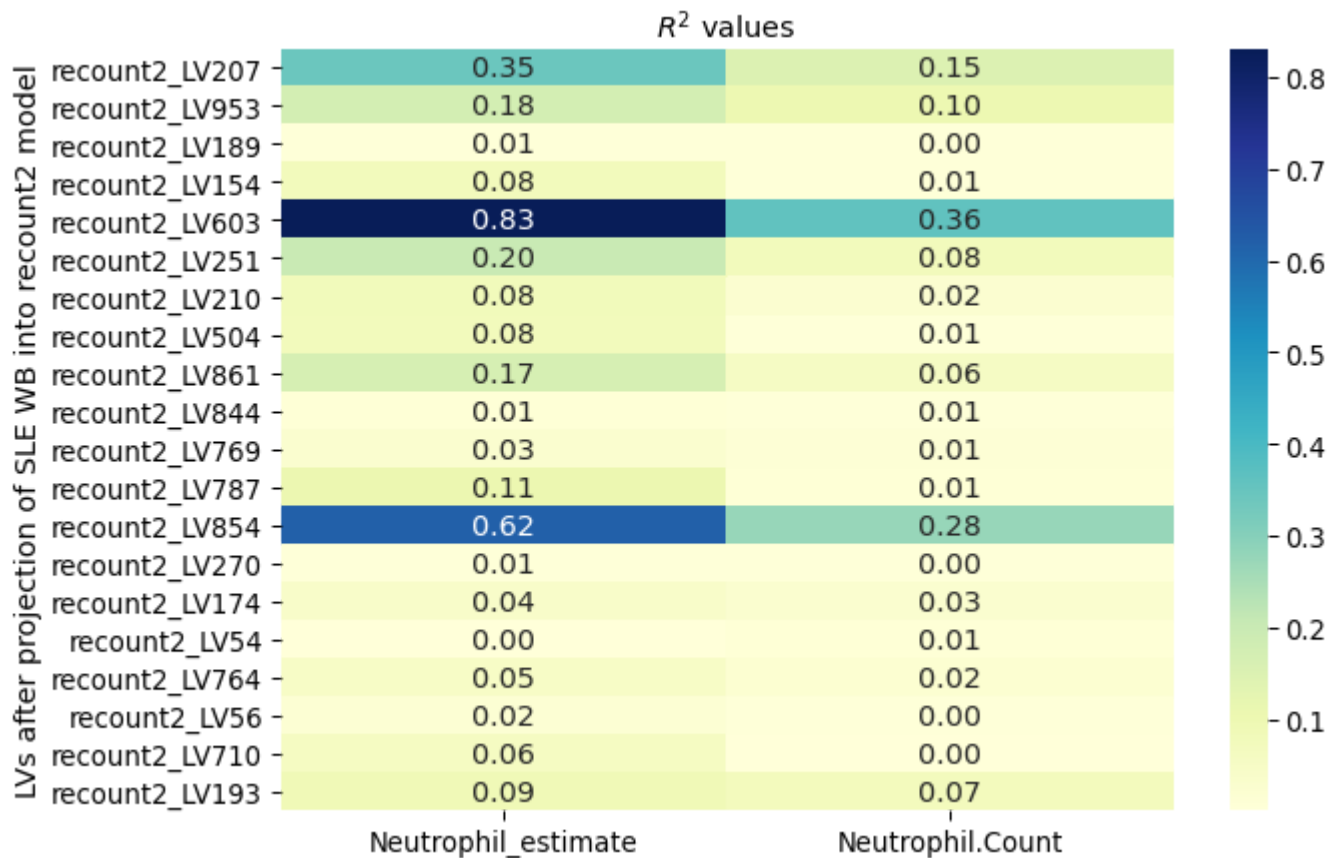


Figure 7: Correlation of neutrophil counts with top LVs associated with neutrophils traits.

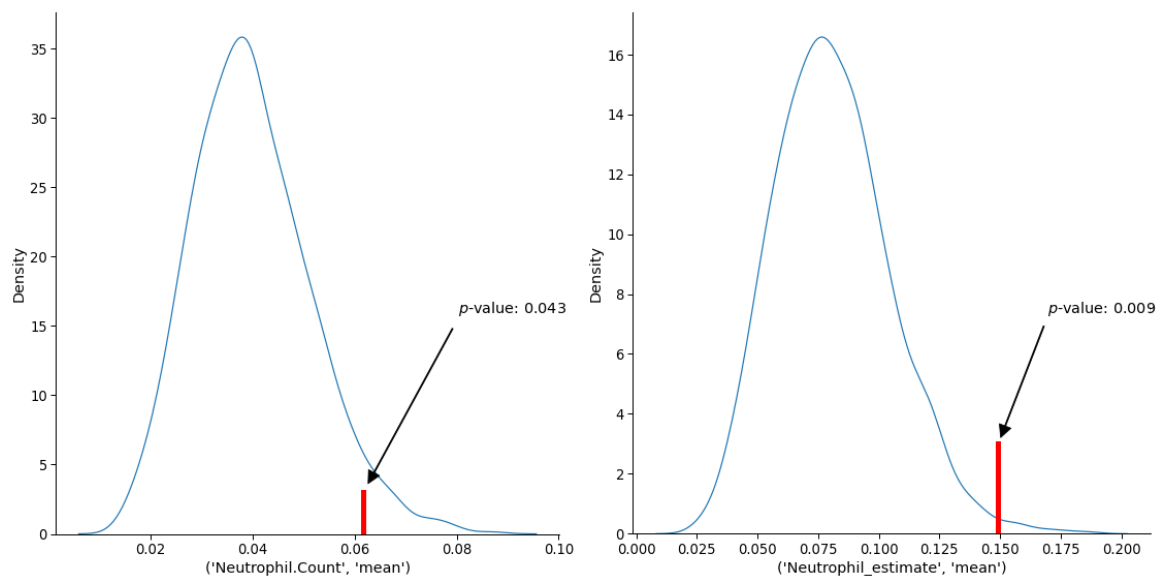


Figure 8: Significance of neutrophil counts correlation.

Consensus clustering of traits in PhenomeXcan

Dimensionality reduction

Ensemble creation: clustering algorithms and parameters

- list of methods and its parameters

Ensemble combination and consensus functions

- evidence accumulation approach
- we also used a spectral clustering approach
- for each k , we picked the partition that maximized the agreement with the ensemble
- show figure where we select the k s that are greater than the median

Clusters interpretation

- we remove each LV and run the decision tree classifier again

Drug-disease predictions

- anti-correlation using dot product of s-predixcan on all tissues and lincs